Essential Readings in Light Metals: Cast Shop for Aluminum Production.
Edited by John F. Grandfield and Dmitry G. Eskin.
© 2013 The Minerals, Metals & Materials Society. Published 2013 by John Wiley & Sons, Inc.

Light Metals — From *Light Metals 1984*, J.P. McGeer, Editor

REMOVAL OF HYDROGEN FROM MOLTEN ALUMINIUM

BY GAS PURGING

T.A. Engh and T. Pedersen

The University of Trondheim
The Norwegian Institute of Technology
Division of Metallurgy
N-7034 Trondheim - NTH,
Norway

Summary.

A model of hydrogen removal from molten aluminium by gas purging is presented. The model includes diffusion of dissolved hydrogen in the melt to the gas bubbles, surface removal, pickup of hydrogen from humidity above the melt and influence of reactive gas.

The theory is compared with measurements taken in laboratory and industrial batch and continuous reactors using lances, porous plugs and spinning nozzles. It is assumed that mass transfer in the melt boundary layer is rate-limiting. The generally accepted mass transfer coefficients have been employed. D_H is taken from a previous paper. Contact areas for the bubbles have been measured in water model experiments and scaled to molten aluminium. The theory gives the ratio end hydrogen/initial hydrogen within limits of ± 15 %. Thus it is possible to calculate purge gas requirements and removal times.

Introduction

Hydrogen is picked up by molten aluminium mainly due to a reaction with H_2O-vapour. Especially for remelted metal it is necessary to reduce hydrogen levels.

Inert gas purging seems to be well suited for the removal due to the high vapour pressure of hydrogen in equilibrium with dissolved hydrogen in molten aluminium

$$\underline{H} = \frac{1}{2} H_2 \qquad (1)$$

A detailed work which compares theory and experimental results will be found in a Ph.D. thesis (1). Here part of this work is presented.

Assumptions

The mathematical description of gas purging is based on the following main assumptions:

a) The bath is well-stirred so that the concentration of $\underline{H}$ is the same throughout the melt.

b) In a horisontal cross-section of the bath hydrogen pressure, p_{H_2}, in the bubbles is the same.

c) Mass transfer of dissolved hydrogen in melt boundary layers (surrounding the bubbles and at the bath surface) is rate limiting.

d) The molten bath is "shallow" (depth less than 1 m) so that we do not have to take the change in total pressure into account. In the calculations we use an average value for the total pressure in the bubbles.

e) The hydrogen partial pressure p_{H_2} is much smaller than the total pressure, p_{total}.

Discussion of assumptions

Assumption a) does not always apply. For instance if there is only one or two porous plugs in a long shallow refining furnace we may not have complete mixing. For a SNIF (Spinning Nozzle Inert Flotation) unit where the impeller diameter is 1/3 of the melt diameter the assumption will be fulfilled. Mixing time (2) will then be very short compared to the time employed in gas purging.

p_{H_2} will depend on bubble diameter (p_{H_2} will be greatest in the small bubbles). Therefore strictly, b) will not be correct if there is a wide distribution of bubble sizes. This case may be worked out introducing the bubble size distribution and bubble rise velocities (for instance obtained from water model experiments). The bubble size distribution is then employed in Eq. 2. The solution becomes rather complicated.

With regard to assumption c) chemical rates may easily be included (for first order kinetics) by introducing total mass transfer coefficients. If diffusion of H_2 in the gas phase must be included, the situation is complicated and it seems, that extensive numerical calculations must be carried out. It seems that variation in total pressure only has to be taken into account for vacuum operation.

Similarly, assumption e) applies for units operating at atmospheric pressure. The reason is that usually H is so low that p_{H_2} << 1 atmosphere.

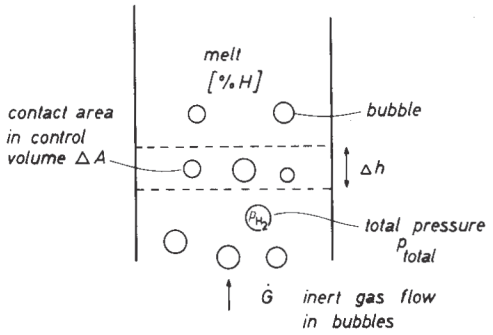

Figure 1 - Control volume of a gas purging reactor.

The hydrogen partial pressure in the bubbles as they escape the bath p_{H_2} is found as follows:

A mass balance for hydrogen over a horisontal slice (see Fig. 1) of the bath gives:

Hydrogen that diffuses into bubbles = increase of hydrogen content of bubbles

or in mathematical form

$$\rho k\,([\%\,H] - [\%\,H]_e)\,\Delta A/(100\cdot m_H) = 2\,\Delta(G\,p_{H_2}/p_{inert}) \qquad (2)$$

Here $[\%\,H] - [\%\,H]_e$ is the driving force for diffusion of hydrogen. $[\%\,H]_e$ is the concentration of hydrogen in the melt in equilibrium with the partial pressure of hydrogen in the bubbles

$$[\%\,H]_e = K\sqrt{p_{H_2}}/f_H \qquad (3)$$

$$[\%\,H]_e \text{ (at bath surface)} = K\sqrt{p^o_{H_2}}/f_H \qquad (3a)$$

If eq. (3) is introduced into (2), we may integrate from bottom to top of the melt giving $p^o_{H_2}$. For this solution reference is made to a previous paper (3). Here the results are presented graphically in Fig. 2 giving dimensionless variable

$$Z = [\%\,H]_e \text{ (at bath surface)}/[\%\,H] \qquad (4)$$

as a function of a dimensionless group

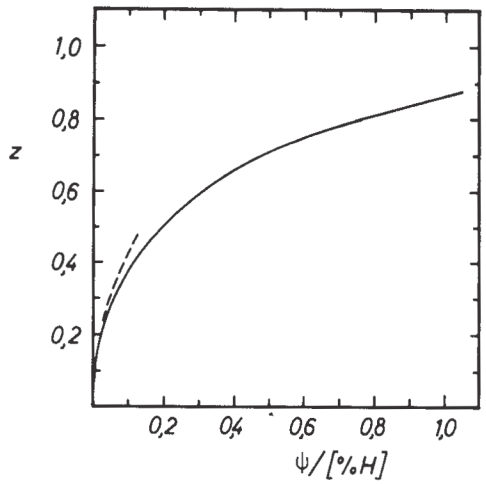

Figure 2 - Dimensionless gas composition, Z, as a function of inverse hydrogen concentration. The limiting solution for diffusion control, $Z^2/2$, is shown by the dashed line.

$$\frac{2\,\psi}{[\%\,H]} = \frac{\text{Maximum hydrogen that can diffuse to bubbles}}{\text{Equilibrium hydrogen content of bubbles}} = \frac{k\cdot A\cdot\rho[\%\,H]/(100\cdot m_H)}{2\,G\cdot p^o_{H_2}/(p_{inert}\cdot Z^2)} = \frac{k\cdot\rho\cdot A\cdot p_{inert}\cdot K^2}{2\,f_H^2\cdot 100\cdot m_H\,G\cdot[\%\,H]} \qquad (5)$$

It is seen that the group is inversely proportional to hydrogen concentration.

If Z < 0.1 we have the diffusion controlled case (3). It Z is close to one (A "large"), chemical equilibrium controls the removal rate. For 0.1 < Z < 0.9 we have a case of mixed control (3). For gas purging with a lance where bubbles size is large, Z has a low value, around 0.1; for a porous plug Z has a somewhat higher values. For a system with a rotating gas impeller Z ∿ 0.7. These systems are compared on Fig. 5.

Equations for hydrogen removal

Once we know the hydrogen content in the escaping bubbles, hydrogen concentrations can be obtained employing a hydrogen mass balance for the refining reactor.

At the top surface hydrogen removal is given by

$$\frac{k_s A_s \rho \left([\%\ H] - [\%\ H]_v\right)}{100 \cdot m_H}$$

See numerical example for $[\%\ H]_v$.

For a "completely exposed" surface $[\%\ H]_v$ is the concentration of hydrogen in the melt given by the equilibrium

$$1/2\ H_2O + 1/3\ Al(\ell) = 1/6\ Al_2O_3(s) + \underline{H} \qquad (6)$$

where p_{H_2O} is the water vapour concentration in the air.

Often the atmosphere above the melt will be protected with a lid so that there should be little or no hydrogen pickup from the air. In this case the gas composition is equal to that of the escaping bubbles so that: $[\%\ H]_v = [\%\ H] \cdot Z$.

By blowing inert gas on the melt surface (combined with a lid), $[\%\ H_v] \approx 0$.

A mass balance equation for a steady-state continuous reactor gives:

Difference between hydrogen flow into and out of reactor = hydrogen removed by bubbles per unit time + hydrogen removal rate at bath surface

or

$$\frac{\dot{M}\left([\%\ H]_i - [\%\ H]\right)}{100 \cdot m_H} = \frac{2\,\dot{G}\,p^o_{H_2}}{p_{inert}} + \frac{\rho\, k_s A_s \left([\%\ H] - [\%\ H]_v\right)}{100 \cdot m_H} \qquad (7)$$

or if eqs. (3) and (4) are introduced

$$\frac{\dot{M}\left([\%\ H]_i - [\%\ H]\right)}{100 \cdot m_H} = \frac{2\,\dot{G}\,f_H^2\,[\%\ H]^2\,z^2}{K^2 \cdot p_{inert}} + \frac{\rho\, k_s A_s \left([\%\ H] - [\%\ H]_v\right)}{100 \cdot m_H} \qquad (8)$$

Using b and B, in the list of symbols eq. (8) can be written:

$$\left([\%\ H]_i - [\%\ H]\right) = + \frac{[\%\ H]^2\, Z^2}{B'} + \frac{b}{B'}\left([\%\ H] - [\%\ H]_v\right) \qquad (9)$$

As mentioned previously Z is given in Fig. 2. $[\%\ H]$ is obtained from eq. (9) as the solution of a simple quadratic equation.

The physical meaning of B' and b may be understood from the following groups:

$$\frac{[\%\ H]}{B'} = \frac{\text{Hydrogen flow in bubbles}}{\text{Hydrogen flowing out in melt}}$$

$$\frac{b}{B'} = \frac{\text{Hydrogen flow out by mass transfer at top surface}}{\text{Hydrogen flowing out in melt}}$$

$$\frac{[\%\ H]}{B} = \frac{\text{Hydrogen flow in bubbles}}{\text{Hydrogen content of melt}}$$

Similarly the mass balance equation for a batch reactor is:

Reduction of content of hydrogen in bath = hydrogen removed by bubbles + hydrogen removed at bath surface

or replacing the lefthand side in eq. (8) with $-\frac{M\, d\,[\%\ H]}{100\ m_H\ dt}$;

B' with B where $\dot{M}$ is replaced by M

$$\frac{d\,[\%\ H]}{dt} = -\frac{[\%\ H]^2 \cdot Z^2}{B} - \frac{b}{B}\left([\%\ H] - [\%\ H]_v\right) \qquad (10)$$

where now Z given by Fig. 2 changes with time since $[\%\ H]$ changes with time. $[\%\ H]$ in Fig. 2 is also given by eq. 11:

$$\psi/[\%\ H] = -Z - \ell n\,(1-Z) \qquad (11)$$

Z is solved numerically by Newton-iteration on eq. (11) or from Fig. 2. Now [% H] is integrated over time by using Runge - Kutta on eq.(10). During the integration corresponding values of [% H] and Z are calculated. Some results are shown in Fig. 5.

Mass transfer coefficients

The mass transfer coefficient to the bubbles is taken from Fig. 4, line d.

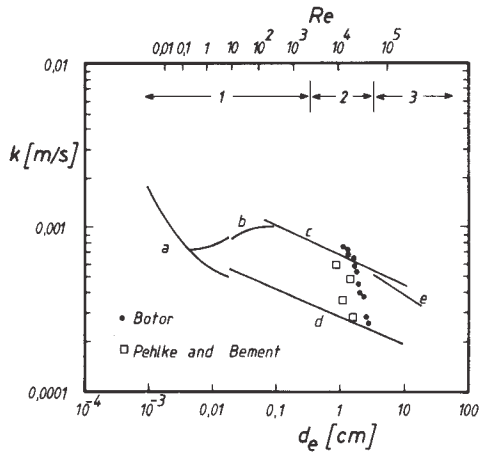

Figure 4 - Predicted and observed mass transfer coefficients for the removal of hydrogen to inert gas bubbles in aluminium at 1000 K. Regimes 1, 2, and 3 correspond to spherical, ellipsoidal, and spherical cap bubbles.
(a) Mass transfer for viscous flow. The upper line is for a freely circulating bubble; the lower is for a rigid bubble. (b) Mass transfer for turbulent flow to a circulating bubble in the transition region. (c) Mass transfer to a circulating bubble in potential flow. (d) Mass transfer to a rigid bubble in potential flow. (e) Mass transfer to the front and rear face of a spherical cap bubble.

The basis for this figure is discussed in a previous paper (3).

Mass transfer to the surface is described for lances and porous plugs using Machlins' equation (4).

$$k_s = \sqrt{\frac{8}{\pi}} \, (U_R \cdot R_c \cdot D_H)^{1/2} / R_c \qquad (12)$$

where U_R is the radial velocity of the metal surface at the crucible edge and R_c is the radius of the crucible.

U_R is obtained using the equation (5):

$$U_R = \left\{ \frac{\dot{Q} \cdot p \cdot \ell n \left(1 + \frac{\rho \cdot g \cdot H}{1.01 \cdot 10^5}\right)}{\pi R_c^2 \cdot \rho} \right\}^{1/3} \qquad (13)$$

where $\dot{Q}$ is the volumetric gas flow in m_N^3/s; p is the pressure equal to 1 atm; ρ is the melt density; g the acceleration of gravity 9.81 m/s^2 and H the bath depth.

For impeller systems $k_{s_{Na}}$ for the removal of dissolved sodium was determined experimentally (6). For hydrogen k_s was then determined using the relation

$$k_s = k_{s_{Na}} \sqrt{\frac{D_H}{D_{Na}}} \qquad (14)$$

Eq (14) is based on the assumption that mass transfer at a "free interface" is proportional to the square root of the diffusion coefficient.

Numerical example

We take batch - gas purging, Run No. 1.3.1. as a numerical example.

AlSi 7 MgO.5 $\quad f_H = 1.75$
($f_H = 1$ for pure Aluminium)

$A = 0.17\ m^2$

$d_b = 26$ mm (measured in water-models (9) and scaled to Aluminium) (1)

$A_s = 0.20\ m^2$

$M = 200$ kg

$\dot{G} = 4.46 \cdot 10^{-6}$ kmols^{-1}

$k = 2.3 \cdot 10^{-4}$ m s^{-1}

$k_s = 1.43 \cdot 10^{-4}$ m s^{-1}

$K = 1.2 \cdot 10^{-4}$

$[\% H]_i = 0.14 \cdot 10^{-4}$ %

$[\% H]_v = 0.14 \cdot 10^{-4}$ % ($[\% H]_v$ is [% H] found in melt after long holding time with no gaspurging. Experimental value is much lower than given by eq. (6) and lower than given by eq. (1) with $p_{H_2} = 1$ atm.)

$B = 1.05\ 10^{-3}$

$b = 3.48\ 10^{-7}$

$\psi = 2.4 \cdot 10^{-7}$

Eqs (10) and (11) are solved by Rhunge-Kutta and plotted as Run No. 1.3.1. in Fig. 5. The symbols + are the experimental values.

Experimental

The batch gas purging experiments were carried out in circular vessels, electrically heated. The SNIF-unit is rectangular in shape. Hydrogen analysis was performed only before and after gas purging in the cast-shops.

The Telegas instrument (7) was employed in all the experiments. It was very important to preheat the probe well, let the probe stay for about 5 min. in the metal while bubbling gas through it and use the mean value of the next three readings. The initial one was discarded since it often gave too high values.

Fig. 6 shows the correspondence between measured and calculated values of end hydrogen for batch refining units. Figs 7a, b, c compare three sets of measured and calculated end values for a continuous refining unit. Also the initial measured values are indicated. Fig. 8 shows the comparison for a system with two units in series.

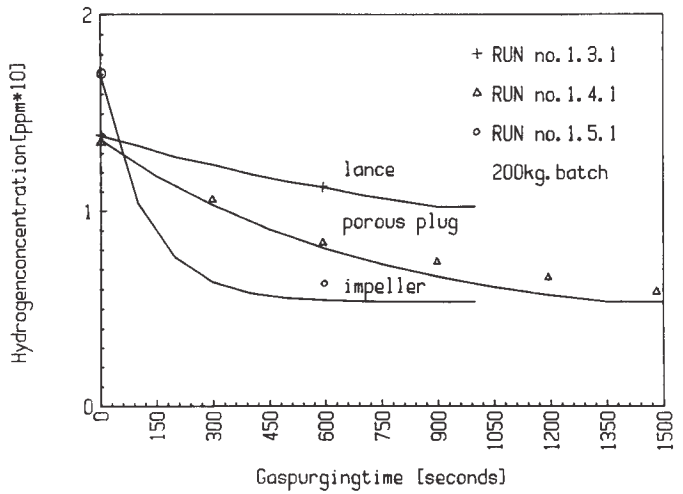

Figure 5 - Gaspurging with lance, porous plug and impeller in 200 kg batch for the same gasflow $\dot{Q} = 0.36\ m^3_N/h$.

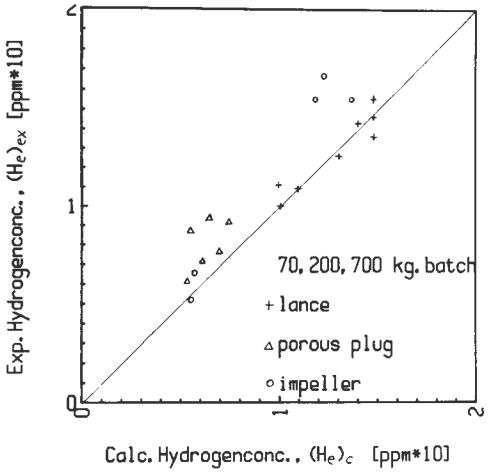

Figure 6 - Experimental and calculated hydrogen concentrations in 70, 200 and 700 kg batch using lances, porous plugs and impellers.

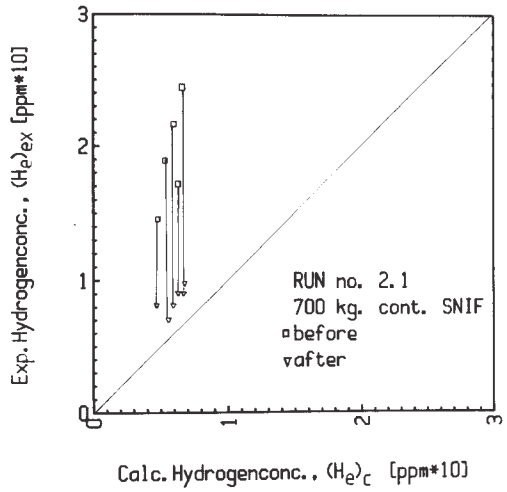

Figure 7a - Experimental and calculated hydrogen concentrations in 700 kg continuous SNIF.

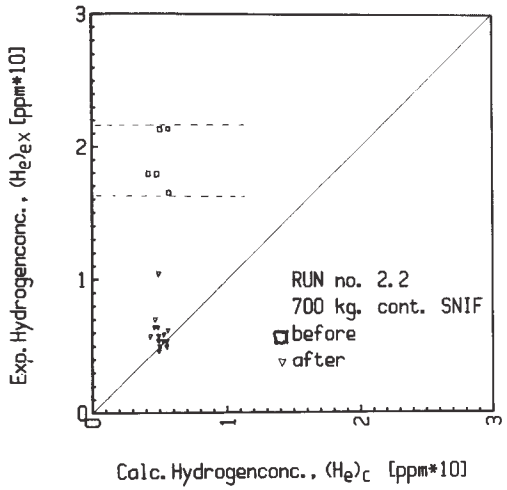

Figure 7b - Experimental and calculated hydrogen concentrations in 700 kg continuous SNIF.

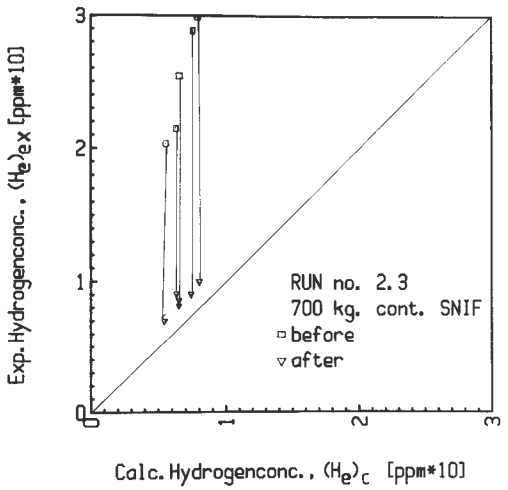

Figure 7c - Experimental and calculated hydrogen concentrations in 700 kg continuous SNIF.

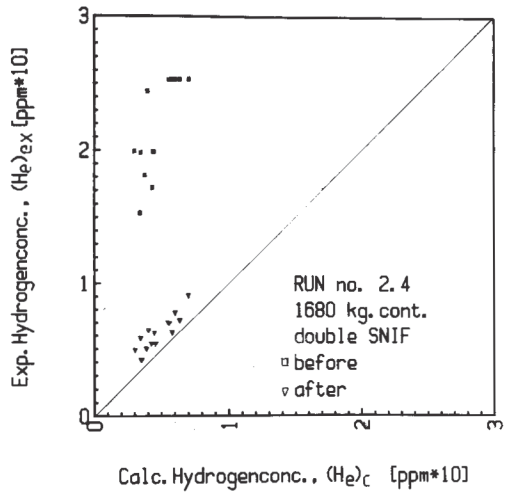

Figure 8 - Experimental and calculated hydrogen concentrations in 1680 kg double continuous SNIF.

Discussion

The measured values tend to be somewhat higher than the calculated values. This may be partly explained by the fact that the telegas instrument tends to give too high readings (1).

From ending the gas purging to reading the telegas instrument there will also be some hydrogen pickup from atmosphere. There will also be some hydrogen pickup from humidity in the refractory-material.

An other factor is that the gas may not be properly dispersed throughout the melt. This occurs if gas flow rates are too high so that "flooding" occurs (9). This effect is illustrated in Fig 9 where the ratio $\frac{H_{exp}}{H_{cal}}$ is given as a function of the total flow rate for a double SNIF.

Furthermore the contact area A inverse proporsional to bubble-radius employed on the calculations is obtained from full scale water-model experiments (9). Our theory (1) indicates that $R_{b,\ melt} \approx 2 \cdot R_{b,\ H_2O}$.

Finally it should be pointed out that the mass transfer coefficients k and k_s are not known very accurately. There are several reasons for this. The mass transfer coefficient is proportional to the square root of the diffusivity of hydrogen, D_H, which is known only roughly. Also k_s is proportional to the square root of the surface velocity which depends on, geometry, position of impeller, etc. Furthermore the surface velocity does not follow the assumptions made in the theory.

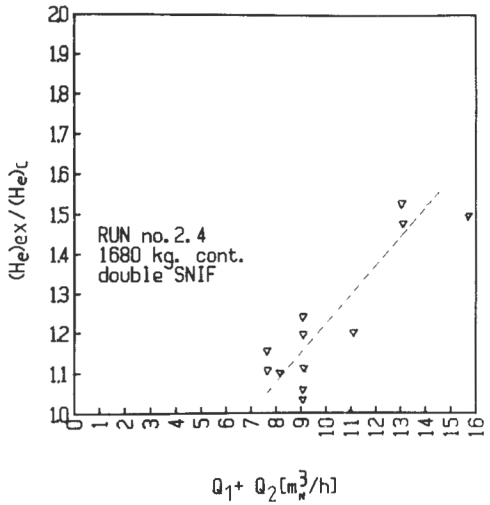

Figure 9 - Ratio between experimental and calculated hydrogen concentrations out of a double continuous SNIF as function of gasflows $\dot{Q}_1$ and $\dot{Q}_2$, showing lower efficiency of the gas at higher flow rates when flooding appears.

"Pickup" of hydrogen from moisture in air may partly be held to low levels by use of a lid.

In Figure 10 is shown theoretical curves for hydrogen removal with (a) surface completely exposed to air with moisture, (b) with a lid and (c) blowing inert gas on the surface. We see from case b in Fig. 10 that a lid greatly improves efficiency. Blowing inert gas on the surface seems to be interesting only if extremely low hydrogen levels are required.

Chlorine in the purge gas will react with Al to $AlCl_3$. It will not react with H to give HCl.

Above the melt $AlCl_3$ may react with H_2O to give Al_2O_3 and HCl. However, HCl should in contact with the bath-surface react according to the scheme

$$3\,HCl + Al = AlCl_3 + 3\,\underline{H}$$

Therefore based on thermodynamic reasoning there seems to be no advantage in the use of Cl_2. However, mass transfer may increase marginally according to Botor (10).

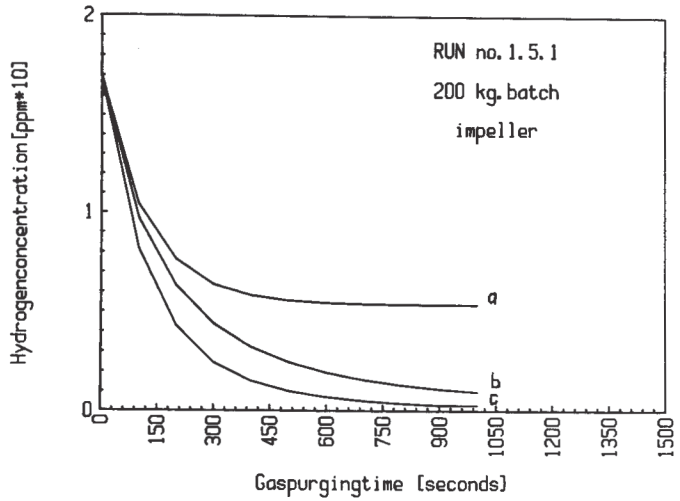

Figure 10 - Calculated curves for hydrogen removal with
a. surface completely exposed against air (as Fig 5)
b. a lid
c. blowing inert gas on the surface (combined with a lid).

Conclusion

A model (1, 3) that gives end or output hydrogen both for batch and continuous inert gas purging units has been checked experimentally both in the laboratory and industrially. Correspondence between calculated hydrogen levels and "Telegas" instrument readings seems acceptable.

For impeller systems operating efficiently hydrogen can be calculated approximately using only the equilibrium between hydrogen in gas and in melt and the inert gas consumption. From the comparison between calculations and measurements or from full-scale water model experiments it is possible to check if "flooding" (large bubbles) reduces efficiency. If flooding occurs, inert gas consumption must be reduced, impeller rotation speed increased or the impeller system should be redesigned.

For the less efficient lance and porous plug systems also the contact areas between gas and melt and mass transfer coefficients must be known in the calculation of hydrogen levels. The contact areas can be measured in full scale water-model experiments and scaled to molten aluminium.

Using a lid to protect the melt against humidity in the air will improve the efficiency.

List of symbols

A	contact area of bubbles in melt $[m^2]$
A_s	contact area of melt surface $[m^2]$
B	$M\ p_{inert} \cdot K^2/(100 \cdot m_H \cdot 2\ f_H^{\cdot 2}\ G)$ $[s]$
b	$\rho \cdot k_s \cdot A_s \cdot p_{inert} \cdot K^2/(100 \cdot m_H \cdot 2\ f_H^{\cdot 2}\ G)$ $[s]$
d_e	equivalent diameter of bubble $[m]$
D_H	diffusivity of hydrogen $[m^2/s]$
E	$\frac{2\ M}{k\ A\ \rho}$
f_H	Henrian activity coefficient of hydrogen
g	acceleration of gravity $[m/s^2]$
G	flow rate of inert gas kg·mole/s
$[\%\ H]$, $[\%\ H]_e$, $[\%\ H]_i$, $[\%\ H]_\infty$	hydrogen concentration, in equilibrium with bubbles, initial and at long times, respectively
k	mass transfer coefficient to bubbles for hydrogen $[m/s]$
k_s	mass transfer coefficients to bath surface for hydrogen $[m/s]$
K	equilibrium constant for hydrogen eq (3)
M	mass of aluminium bath $[kg]$
m_H	molecular weight of hydrogen
p_{inert}	pressure of inert gas $[atm]$
p_{H_2}	pressure of H_2 in bubbles $[atm]$
$p^o_{H_2}$	pressure of H_2 in bubbles at melt surface $[atm]$
p_{total}	total pressure $[atm]$
ρ	density of melt $[kg/m^3]$
R	gas constant 1.9873 kcal/kmole K
R_b	radius of gas bubbles $[m]$
R_c	radius of vessel $[m]$
t	time from start of gas purging $[s]$
U_R	surface velocity $[m/s]$
Z	square root of $p^o_{H_2}$ to the equilibrium value
ψ	$\frac{k \cdot A \cdot p_{inert} \cdot K^2}{4\ f_H^{\cdot 2} \cdot 100\ m_H \cdot G}$.

B' is found from B by replacing M with M.

Acknowledgement

The authors wish to acknowledge gratefully the financial support of the Royal Norwegian Council for Scientific and Industrial Research under project MK 0520.09808 which makes this research possible.

References

(1) T. Pedersen, Ph.D. thesis, to be published.

(2) S. Asai, T. Okomoto, J.C. He, and I. Muchi, "Mixing time of refining vessels stirred by gas injection," Trans ISIJ, 23 (1983) pp. 43-50.

(3) G.K. Sigworth, and T.A. Engh, "Chemical and Kinetic factors related to hydrogen removal from Aluminium," Metallurgical Trans. B, 13B, (1982) pp. 447-460.

(4) F.D. Richardson, Physical Chemistry of Melts in Metallurgy, Vol. 2, pp. 477-487, Academic Press, New York, N.Y., 1974.

(5) T.A. Engh, and S.T. Johansen, "Convection and Stirring Induced by Bubbling from a Porous Plug," Proceedings of the Shanghai Symposium on Injection Metallurgy, Nov. 1982, Shanghai, China.

(6) T. Pedersen, "Fjerning av lettelementene Na, Li og Ca ved spylgass-behandling og røring,"STF34 A83014, SINTEF, NTH, Trondheim, 1983.

(7) C.E. Ramsley, and D.E.I. Talbot, "An instrument for measuring the gas content of Aluminium alloy during melting and casting," Journal of the Institute of Metals 86, (1957-58) pp. 212-219.

(8) S. Nagata, "Mixing, Principles and Applications", Kodansha Ltd., 1975.

(9) B. Rasch, "Bestemmelse av boblestørrelse og kontaktareal gass/væske ved hjelp av vannmodell-forsøk", STF34 A82094 SINTEF, NTH, Trondheim, 1982.

(10) J. Botor, "Kinetics of hydrogen-degassing of molten Aluminium by purge gas," Aluminium,56 (8) (1980) pp. 519-522.